Available online at www.sciencedirect.com

ScienceDirect

Ceramics International 40 (2014) 16141–16146

CERAMICS INTERNATIONAL

www.elsevier.com/locate/ceramint

Sol–gel combustion synthesis of Zr-doped $BaTiO_3$ nanopowders and ceramics: Dielectric and ferroelectric studies

M. Aghayan[a], A. Khorsand Zak[b,c,*], M. Behdani[a], A. Manaf Hashim[c]

[a]Department of Physics, Faculty of Science, Ferdowsi University of Mashhad, Mashhad, Iran
[b]Nanotechnology Laboratory, Esfarayen University of Technology, Esfarayen 96619-98195, North Khorasan, Iran
[c]Malaysia-Japan International Institute of Technology, Universiti Teknologi Malaysia, Jalan Semarak, 54100 Kuala Lumpur, Malaysia

Received 18 June 2014; received in revised form 8 July 2014; accepted 8 July 2014
Available online 15 July 2014

Abstract

The dielectric and ferroelectric properties of the ceramic system, $Ba(Ti_{1-x},Zr_x)O_3$, were investigated for compositions $0 \le x \le 0.2$. The primary nanopowders were synthesized using a sol–gel combustion route to obtain the homogenous compounds. X-ray diffraction patterns demonstrated that there was a cubic structure for the prepared nanopowders. The nanopowders were pressed into pellet form and sintered at 1250, 1300, and 1350 °C. The results revealed a significant increase in the permittivity of the Zr-doped samples. The sample showed the best dielectric properties and a ferroelectric behavior for the value of $x=0.05$.

Keywords: $BaTiO_3$; Barium titanate; Nanoparticles; Nanopowders; Dielectric

1. Introduction

Barium titanate ($BaTiO_3$) is an environment-friendly dielectric and ferroelectric materials with similar performance as many Pb-based electro-ceramics [1]. Due to its high dielectric constant, it is widely utilized to manufacture electronic components such as multilayer ceramic capacitor (MLCC), Micro-Electro Mechanical Systems (MEMs), Dynamic Random Access Memories (DRAM), PTC thermistors, piezoelectric transducers, and a variety of electro-optic devices [2–4].

Micrometer $BaTiO_3$ undergoes a paraelectric to ferroelectric phase transition at about T_c =130 °C, which is accompanied by a sharp peak in the permittivity curve. Above the Curie temperature, the structure of barium titanate is cubic and paraelectric. Below the Curie point, the structure is slightly distorted and three ferroelectric phase with nonzero dipole moment exist depending on temperature. The tetragonal is stable between ~10 °C and 130 °C. Below 10 °C the structure becomes orthorhombic and a further transition to rhombohedral structure occurs at −80 °C [5]. In tetragonal phase, the ratio of the lattice constant (*c*/*a*) has been shown to decrease as the particle size decreases [6]. Therefore, by controlling the grain size, the dielectric and ferroelectric properties of the ceramics will be changed. It was found that the dielectric permittivity is increased by the grain size decreases [7]. Using nanopowders as source to prepare ceramics pellet is one of the ways to control the growing of the ceramics grains. So the grain size of ceramic layer should be controlled to be small enough. Since the permanent polarization disappears above the Curie temperature, the control of T_c in ferroelectric materials is of great importance for practical applications [8]. Recently, Ba$(Zr_xTi_{1-x})O_3$ (BZT) has been chosen for the fabrication of ceramic capacitors because Zr^{4+} is chemically more stable than Ti^{4+} [9]. In addition, Zr-substitution at Ti-site has been found to be an effective way to decrease the Curie temperature and exhibited several interesting features in the dielectric behavior of $BaTiO_3$ ceramics [10]. The nature of the ferroelectric phase transition at the Curie temperature T_c of BZT is known to change strongly with the Zr content. At higher Zr contents ($x > 0.08$), BZT ceramics show a broad dielectric constant-temperature curve near T_c; caused by

*Corresponding author. Tel.: +60 162017558, +98 9155021785.
E-mail address: alikhorsandzak@gmail.com (A. Khorsand Zak).

http://dx.doi.org/10.1016/j.ceramint.2014.07.045
0272-8842/

inhomogeneous distribution of Zr ions on Ti sites and mechanical stress in the grain [9].

In this work, $Ba(Zr_xTi_{1-x})O_3$ (BZT) nanopowders ($x=0.0$, 0.05, 0.1, 0.15, and 0.2) were synthesized by a sol–gel combustion method at different calcinations temperatures to obtain a single phase powders. The effect of the sintering temperature on the ferro- and dielectric properties of the prepared pellets using the nanopowders were investigated.

2. Experimental

The starting materials used in this experiment were barium nitrate ($Ba(NO_3)_2$, 99% Sigma-Aldrich), zirconium oxynitrate ($ZrO(NO_3)_2 \cdot xH_2O$, 99% Sigma-Aldrich), and titanium(IV) isopropoxide ($Ti[OCH(CH_3)_2]_4$, 97% Sigma-Aldrich). The proper material amounts were calculated according to the following reaction relationship:

$$Ba(NO_3)_2 + x \times [ZrO(NO_3)_2 \times xH_2O] + (1-x) \times Ti\left(OCH(CH_3)_2\right)_4 \rightarrow Ba(Zr_x, Ti_{(1-x)})O_3 + \cdots$$

where: $y=0$, 0.05, 0.1, 0.15, and 0.2.

The process involved many steps.First, an aqueous solution for each cation (Ba^{+2}, Zr^{+4}) was prepared by dissolving barium nitrate and zirconium nitrate in a minimum amount of distilled water at 40 °C. The appropriate amount of titanium (IV) isopropoxide was then dissolved in a mixture of nitric and citric acid for the preparation of the Ti^{+4} solution. The acid amount calculations were conducted as follows [11]:

$$\frac{\text{citric}-\text{acid}}{\text{metal}-\text{cation}} = \frac{2}{5} \quad , \quad \frac{\text{nitric}-\text{acid}}{\text{citric}-\text{acid}} = 1$$

The prepared barium and zirconium solutions were added to the titanium aqueous solution while continuously stirring it at 55–60 °C until the pH of the solution reached 7 by the addition of ammonium hydroxide. The clear obtained sol was refluxed for 2 h at 110 °C and then heated at approximately 80 °C to evaporate all of the water and obtain a clear and viscose gel. Finally, the nitric acid was added to the gel for the cobution process; this resulted in the creation of a xerogel powder. After the auto-combustion process, the resultant xerogel powders were calcined at 700, 800, 900, and 1000 °C to obtain the desired single-phase BZT powders. The resulting nanopowders were mixed thoroughly with the PVA binder solution and pressed into disk pellets under a pressure of 20 MPa. The prepared pellets were sintered at 1250, 1300, and 1350 °C for 6 h in air.

The phase evaluations of the synthesized nanopowders were studied using a powder X-ray diffractometer (XRD, Philips, X'pert, Cu $K\alpha$). Both a scanning and a transition electron microscope (TEM, Leo 912AB, Germany) were used to study the morphology of the synthesized samples. The temperature dependence of the relative permittivity (ε_r) of the samples was measured using an impedance analyzer (HP 4192A Impedance

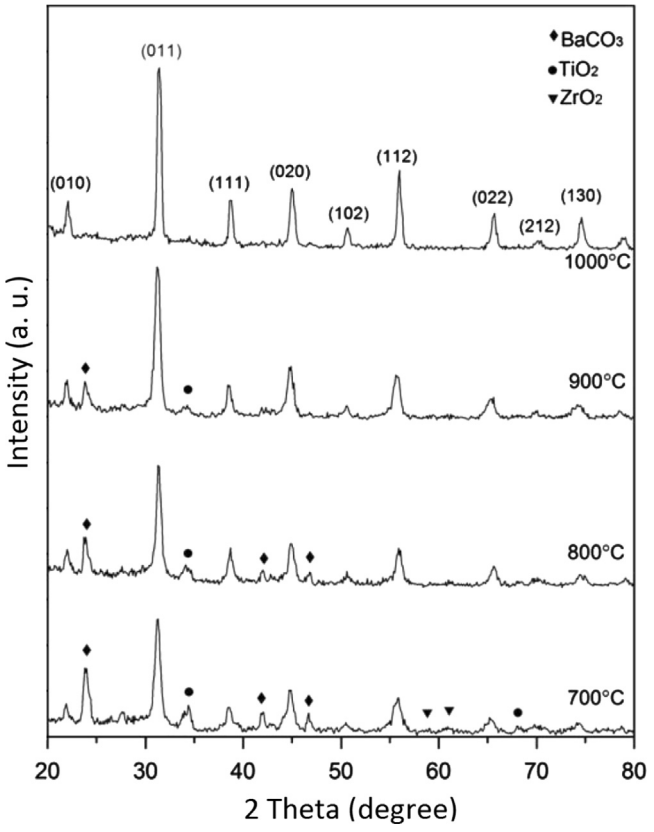

Fig. 1. XRD pattern of Ba $(Zr_{0.05}Ti_{0.95})O_3$ nanopowders obtained at different calcinations temperatures of 700, 800, 900, and 1000 °C.

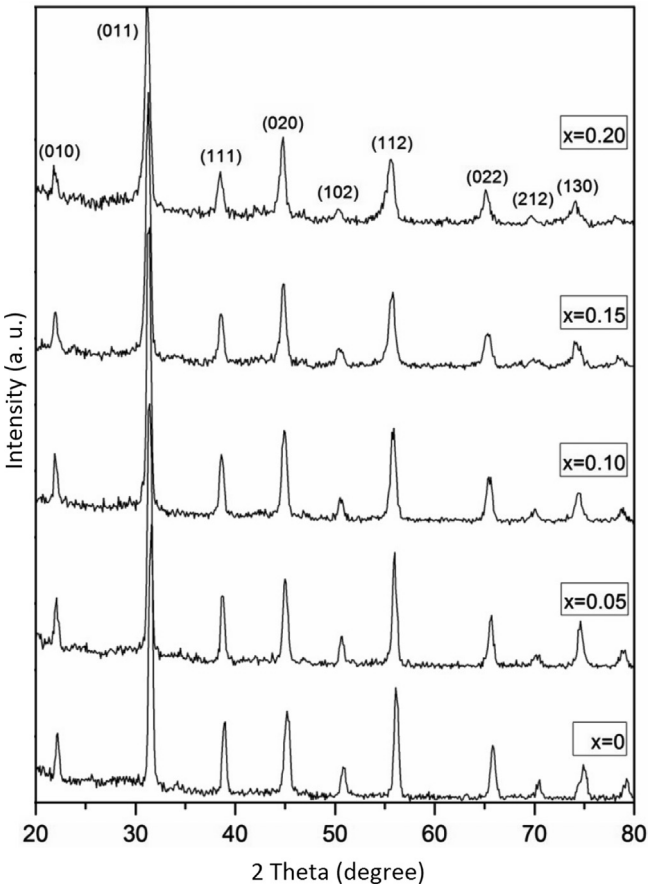

Fig. 2. XRD patterns of Ba $(Zr_xTi_{1-x})O_3$ nanopowders for $x=0$, 0.05, 0.1, 0.15, and 0.2.

Analyzer) at different frequencies, from 1 kHz to 1 MHz. The polarizations versus the electric field hysteresis loops were determined at 50 Hz in silicone oil, using a modified Sawyer Tower circuit.

3. Results and discussion

3.1. Structural studies

Fig. 1 illustrates the X-ray diffraction pattern of the BZT ($x=0.05$) powders calcinated at different temperatures of 700, 800, 900, and 1000 °C for 6 h. At temperatures lower than 1000 °C, some diffraction peaks were detected. This is related to the $BaCO_3$, ZrO_2 and TiO_2 compounds. After 1000 °C, the diffraction peaks completely disappeared and a single phase BZT was achieved.

It is evident that the sample has a perovskite structure with a cubic phase (JCPDS file no. 31-0174). This result concurs with the results of other studies [12]. Frey and Payne reported that 35 nm $BaTiO_3$ particles have cubic symmetry, while grain growth to 100 nm and beyond leads to a slight lattice distortion

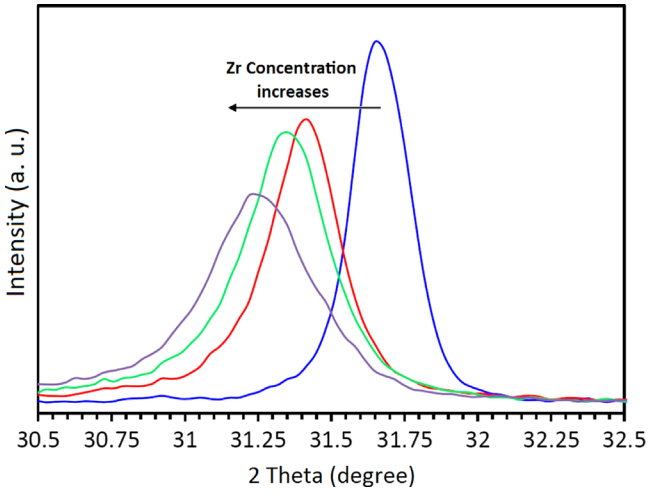

Fig. 3. The shift of (0 1 1) diffraction peak due to the substituting of Ti ions by Zr ions.

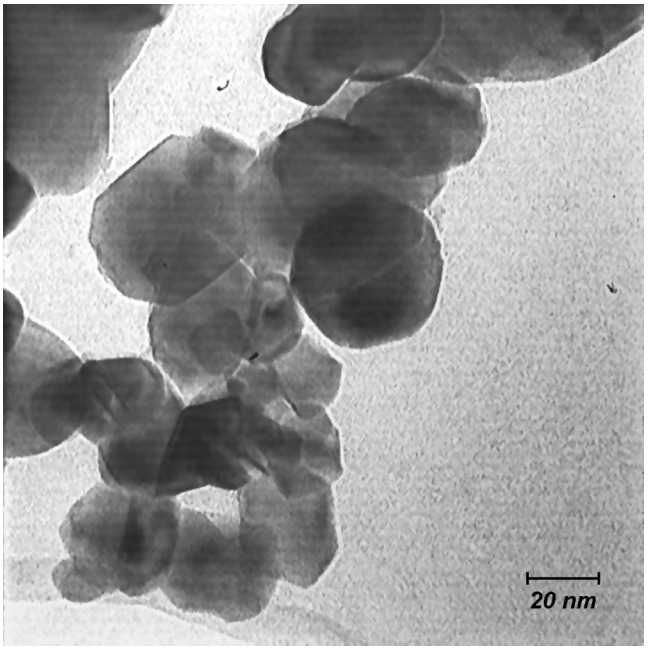

Fig. 4. TEM image of Ba $(Zr_{0.05}Ti_{0.95})O_3$ nanopowders.

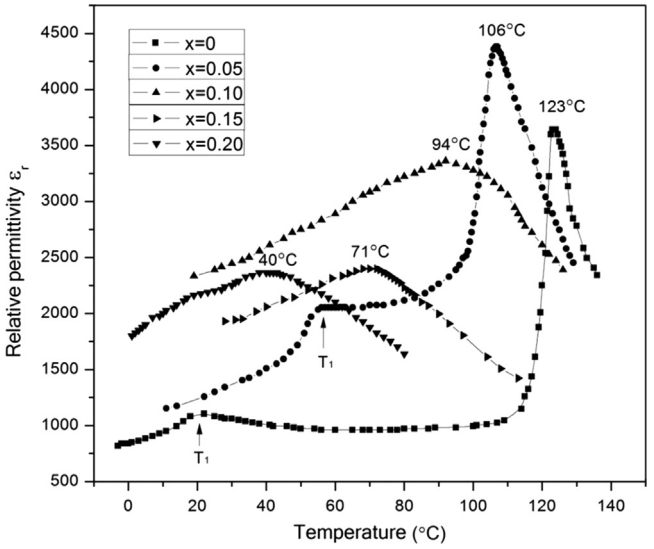

Fig. 5. The variations of permittivity vs. temperature for Ba $(Zr_xTi_{1-x})O_3$ samples.

Table 1
The phase transition temperatures for Ba $(Zr_xTi_{1-x})O_3$ samples.

Ba $(Zr_xTi_{1-x})O_3$	T_1	T_c
$X=0.0$	20	123
$X=0.05$	56	106
$X=0.1$	–	94
$X=0.15$	–	71
$X=0.2$	–	40

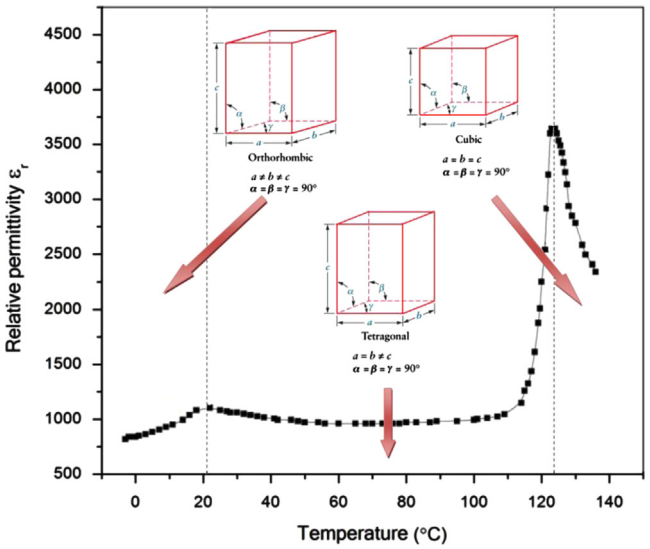

Fig. 6. The different structures corresponding to the each temperature region.

readily detectable by XRD [13]. Kwon and Yoon showed that tetragonality increases linearly with the average particle size, up to 330 nm [14].

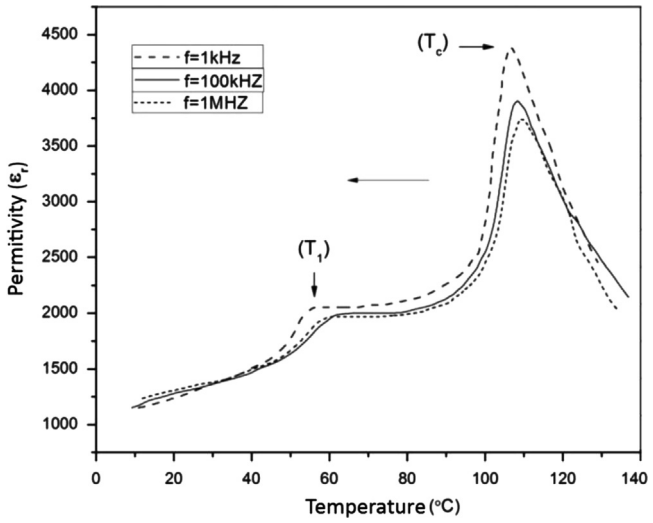

Fig. 7. The variation of the permittivity of Ba $(Zr_{0.05}Ti_{0.95})O_3$ sample vs. temperature at measured at different frequencies.

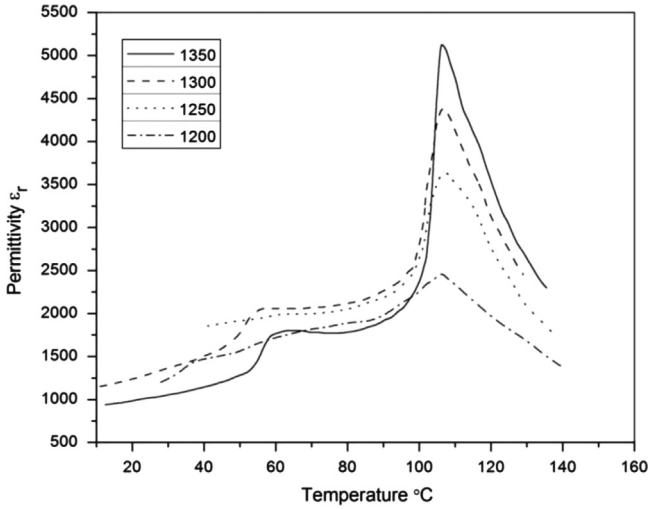

Fig. 8. The variation of the permittivity of Ba $(Zr_{0.05}Ti_{0.95})O_3$ sample sintered at different temperatures vs. temperature.

Fig. 2 illustrates the XRD patterns of the BZT nanopowders with various Zr/Ti ratios, calcinated at 1000 °C. It is evident that all samples have a perovskite cubic structure without extra phases related to the other compounds and impurities. Moreover, it was observed that the diffraction peaks shifted to the lower angles with an increase in the Zr content, Fig. 3. This can be attributed a Zr^{+4} ionic radius (0.087 nm) that is larger than that of Ti^{+4} (0.068 nm)[10,15]. Thus, the substitution of Ti^{+4} by Zr^{+4} could increase the lattice constant.

The typical TEM image of the synthesized BZT nanopowders, with 5% of Zr, calcinated at 1000 °C, is illustrated in Fig. 4. The average particle size of the BZT nanoparticles was found to be approximately 25 nm in diameter with an average grain size of 2 μm for the ceramics after sintering the powder pellet at 1350 °C for 6 h.

3.2. Temperature dependence of the dielectric and ferroelectric properties

The temperature dependence of the relative permittivity of $Ba(Zr_xTi_{1-x})O_3$ ceramics with various Zr contents ($x=0$, 0.05, 0.1, 0.15, and 0.2) are shown in Fig. 5. It was found that the maximum value, corresponding to the Curie temperature, T_c, (the phase transition temperature of cubic paraelectric to tetragonal ferroelectric), decreases as the Zr/Ti ratio increases (Table 1). Since the radius of the Zr^{+4} ion (0.087 nm) is larger than the Ti^{+4} ion (0.068 nm), substitution of Zr^{+4} for Ti^{+4} will weaken the bonding forces between the B-site and the oxygen ions in the ABO_3 perovskite structure. As the B–O bonds weaken, the B-site ion can resume its position so the phase transition temperature can be reduced, but only when the tetragonal ferroelectric is at a lower temperature [15]. Moreover, the dielectric constant of the BZT ceramics with a higher Zr content exhibit broad peaks. This is caused by an inhomogeneous distribution of the Zr ions on the Ti sites and the mechanical stress in the grain [9].

Another dielectric peak, apart from the T_c peak, is clearly noticeable, especially for the composition of $x=0$ and 0.05. This peak is related to the transition temperature from the tetragonal to the orthorhombic structure (T_1), which is also a ferroelectric to ferroelectric phase transition (Fig. 6). This peak (T_1) shifts toward higher temperatures as the Zr content

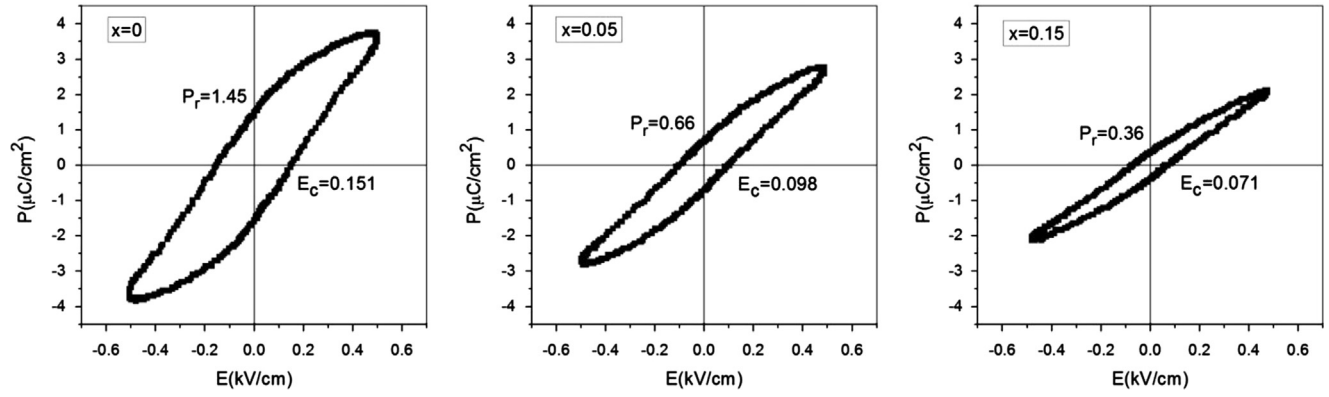

Fig. 9. The hysteresis loops for Ba $(Zr_xTi_{1-x})O_3$ samples ($x=0$, 0.05, and 0.15).

increases. Fig. 7 illustrates the relative permittivity of BZT with 5% of Zr with respect to temperature at different frequencies of 1 kHz, 100 kHz, and 1 MHz. By increasing the frequencies, the value of T_c shifted towards a higher temperature; this was due to the greater dimensional freedom of the dipoles at higher temperatures [1]. In addition, the permittivity of the BZT ceramics with 5% of Zr sintered at different temperatures of 1200 to 1350 °C was measured with respect to the temperature (Fig. 8). The response of the permittivity to the temperature of the samples increased as the sintering temperature increased, resulting in a lower number of the disorders.

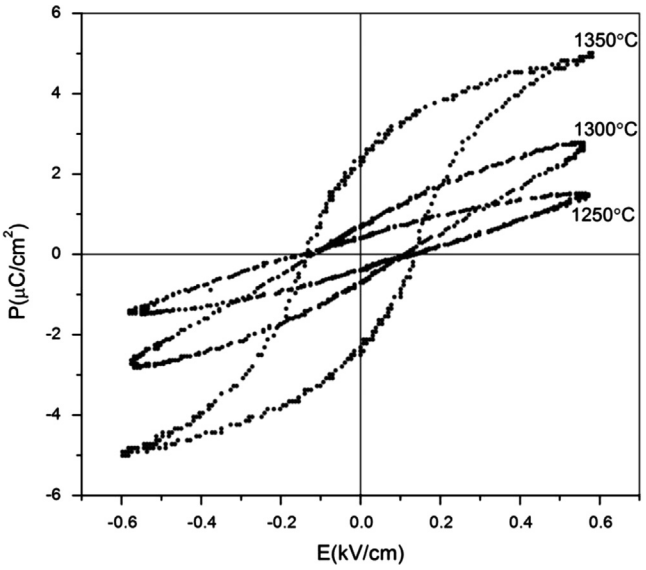

Fig. 10. The hysteresis loops for Ba $(Zr_{0.05}Ti_{0.95})O_3$ samples sintered at different temperatures.

3.3. Hysteresis loop

The ferroelectric hysteresis loops (P versus E) for the prepared $Ba(Zr_x, Ti_{1-x})O_3$ samples for $x=0.0$, 0.05, and 0.15 sintered at 1300 °C are shown in Fig. 9. It was observed that the remnant polarization (P_r) decreased from 1.45 to 0.36 (μC/cm^2). Consequently, substituting Ti ions with Zr ions decreases the ferroelectric behavior of the barium titanate.

In the previous section, it was determined that the sample that contained 5% zirconium illustrated a better dielectric behavior. Therefore, the effect of the sintering temperature on the ferroelectric properties of the prepared $Ba(Zr_{0.05}, Ti_{0.95})O_3$ were studied. Fig. 10 shows the hysteresis loops of the BZT ceramics at room temperature, sintered at 1250–1350 °C for 6 h. It is evident that remanent polarization increases from 0.4 to 2.3 (μC/cm^2) as the sintering temperature increases. This may be due to the growth of the ceramic grains in the higher sintering temperatures, which results in bigger dipoles.

To complete the ferroelectric studies, the remnant polarizations and the corresponding hysteresis loops of the sample with 5% zirconium sintered at 1350 °C were measured from room temperature to its Curie temperatures. It was found that remnant polarization (P_r) first increases and then decreases as temperature increased.

The remnant polarization versus the temperature is illustrated in Fig. 11. As the temperature increases, the spatial dependence of the dipoles decreases, and hence, they become relaxed. As such, the dipoles can follow the electric field easier, resulting in an increase in P_r. A further increase in the temperature causes the structure to tend towards a cubic structure. The size of the dipole moment gradually decreases and P_r approaches zero at the Curie temperature. The values of the P_r and E_c at different temperatures are presented in Fig. 12.

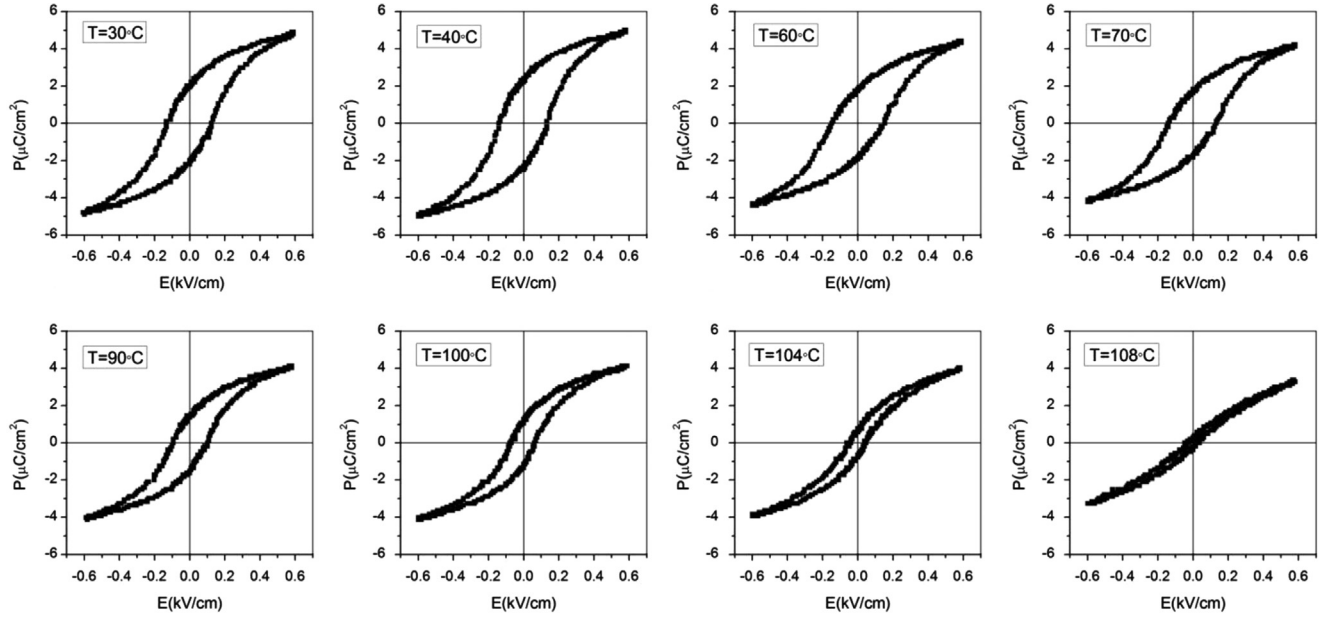

Fig. 11. The hysteresis loops for Ba $(Zr_{0.05}Ti_{0.95})O_3$ samples measured at different temperatures.

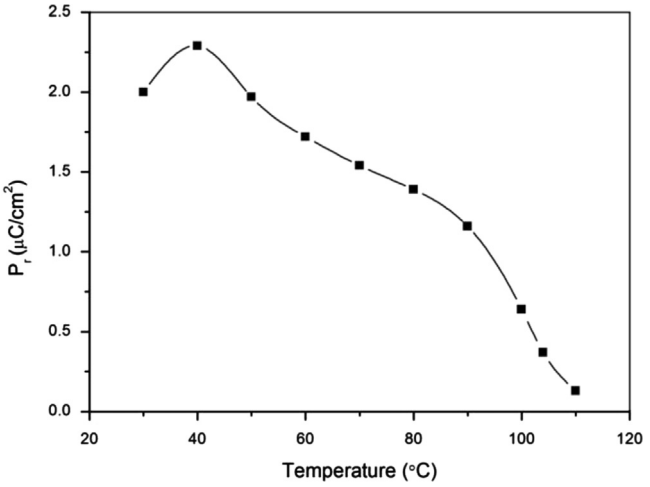

Fig. 12. The value of remnant polarization (P_r) for Ba ($Zr_{0.05}Ti_{0.95}$)O_3 samples measured at different temperatures.

4. Conclusions

Zr-doped $BaTiO_3$ nanopowders were synthesized using a sol–gel combustion method. The synthesized nanopowders were characterized and then pressed into pellet form. The prepared pellets were sintered at different temperatures of 250, 1300, and 1350 °C for 6 h. The dielectric and ferroelectric properties of the prepared ceramics were investigated. The results showed that the permittivity of $BaTiO_3$ increased with substitutions of Ti by Zr ions; whereas, the ferroelectric behavior decreased. Based on the obtained results, Ba($Ti_{0.95}$, $Zr_{0.05}$)O_3 illustrated higher permittivity when compared to $BaTiO_3$; it also demonstrated a good ferroelectric property.

Acknowledgements

A. Khorsand Zak thanks Universiti Teknologi Malaysia for the post-doctoral fellowship. This work was partly funded by Universiti Teknologi Malaysia. Also, M. Behdani thanks Ferdowsi University of Mashhad for the grant support.

References

[1] C. Ciomaga, M. Viviani, M. Buscaglia, V. Buscaglia, L. Mitoseriu, A. Stancu, P. Nanni, Preparation and characterisation of the Ba (Zr, Ti) O3 ceramics with relaxor properties, J. Eur. Ceram. Soc. 27 (13-15) (2007) 4061–4064.

[2] I. Battisha, A. Abou Hamad, R. Mahani, Structure and dielectric studies of nano-composite Fe_2O_3:$BaTiO_3$ prepared by sol–gel method, Physica B 404 (16) (2009) 2274–2279.

[3] K. Sadhana, T. Krishnaveni, K. Praveena, S. Bharadwaj, S. Murthy, Microwave sintering of nanobarium titanate, Scr. Mater. 59 (5) (2008) 495–498.

[4] W. Chaisan, R. Yimnirun, S. Ananta, Effect of vibro-milling time on phase formation and particle size of barium titanate nanopowders, Ceram. Int. 35 (1) (2009) 173–176.

[5] Z. Zhao, V. Buscaglia, M. Viviani, M.T. Buscaglia, L. Mitoseriu, A. Testino, M. Nygren, M. Johnsson, P. Nanni, Grain-size effects on the ferroelectric behavior of dense nanocrystalline BaTiO_ {3} ceramics, Phys. Rev. B: Condens. Matter 70 (2) (2004) 24107.

[6] X. Li, W.H. Shih, Size effects in barium titanate particles and clusters, J. Am. Ceram. Soc. 80 (11) (1997) 2844–2852.

[7] A. Zak, A. Jalalian, S. Hosseini, A. Kompany, N. Shekofteh, Effect of Y 3 and Nb 5 co-doping on dielectric and piezoelectric properties of PZT ceramics, Mater. Sci.-Poland 28 (3) (2010).

[8] S. Tsukada, Y. Akishige, Marked increase in Curie temperature upon annealing of Ferroelectric KF-substituted barium titanate, Scr. Mater. (2010).

[9] X. Tang, J. Wang, X. Wang, H. Chan, Effects of grain size on the dielectric properties and tunabilities of sol–gel derived Ba ($Zr_{0.2}Ti_{0.8}$) O_3 ceramics, Solid State Commun. 131 (3-4) (2004) 163–168.

[10] N. Nanakorn, P. Jalupoom, N. Vaneesorn, A. Thanaboonsombut, Dielectric and ferroelectric properties of Ba (Zr_xTi_{1-x}) O_3 ceramics, Ceram. Int. 34 (4) (2008) 779–782.

[11] G.H. Khorrami, A. Khorsand Zak, A. Kompany, Optical and structural properties of *X*-doped (*X*=Mn, Mg, and Zn) PZT nanoparticles by Kramers–Kronig and size strain plot methods, Ceram. Int. 38 (7) (2012) 5683–5690.

[12] T. Tsurumi, T. Hoshina, H. Takeda, Y. Mizuno, H. Chazono, Size effect of barium titanate and computer-aided design of multilayered ceramic capacitors, IEEE Trans. Ultrason. Ferroelectr. Freq. Control 56 (8) (2009) 1513–1522.

[13] M. Frey, D. Payne, Grain-size effect on structure and phase transformations for barium titanate, Phys. Rev. B: Condens. Matter 54 (5) (1996) 3158–3168.

[14] S.W. Kwon, D.H. Yoon, Effects of heat treatment and particle size on the tetragonality of nano-sized barium titanate powder, Ceram. Int. 33 (7) (2007) 1357–1362.

[15] S. Kuang, X. Tang, L. Li, Y. Jiang, Q. Liu, Influence of Zr dopant on the dielectric properties and Curie temperatures of Ba (Zr_xTi_{1-x}) O_3 ($0 <= x <= 0.12$) ceramics, Scr. Mater. 61 (1) (2009) 68–71.